JOURNAL OF VIROLOGY, June 2006, p. 5992–6002 Vol. 80, No. 12
0022-538X/06/$08.00+0 doi:10.1128/JVI.02680-05

Biochemical Activities of Highly Purified, Catalytically Active Human APOBEC3G: Correlation with Antiviral Effect

Yasumasa Iwatani,[1] Hiroaki Takeuchi,[2] Klaus Strebel,[2] and Judith G. Levin[1]*

Laboratory of Molecular Genetics, National Institute of Child Health and Human Development,[1] and Laboratory of Molecular Microbiology, National Institute of Allergy and Infectious Diseases,[2] Bethesda, Maryland 20892

Received 21 December 2005/Accepted 4 April 2006

APOBEC3G (APO3G), a cytidine deaminase with two zinc finger domains, inhibits human immunodeficiency virus type 1 replication in the absence of Vif. Here, we provide a comprehensive molecular analysis of the deaminase and nucleic acid binding activities of human APO3G using a pure system containing only one protein component, i.e., highly purified, catalytically active enzyme expressed in a baculovirus system. We demonstrate that APO3G deaminates cytosines in single-stranded DNA (ssDNA) only, whereas it binds efficiently to ssDNA and ssRNA, about half as well to a DNA/RNA hybrid, and poorly to double-stranded DNA and RNA. In addition, the base specificities for deamination and binding of ssDNA are not correlated. The minimum length required for detection of APO3G binding to an ssDNA oligonucleotide in an electrophoretic mobility shift assay is 16 nucleotides. Interestingly, if nucleocapsid protein and APO3G are present in the same reaction, we find that they do not interfere with each other's binding to RNA and a complex containing the RNA and both proteins is formed. Finally, we also identify the functional activities of each zinc finger domain. Thus, although both zinc finger domains have the ability to bind nucleic acids, the first zinc finger contributes more to binding and APO3G encapsidation into virions than finger two. In contrast, deamination is associated exclusively with the second zinc finger. Moreover, zinc finger two is more important than finger one for the antiviral effect, demonstrating a correlation between deaminase and antiviral activities.

Human immunodeficiency virus type 1 (HIV-1) requires a virus-encoded gene product, Vif (originally called "Sor" or "A") (8, 43), to replicate efficiently in primary human lymphocytes, monocytes, and certain T-cell lines (e.g., H9), which are commonly designated "nonpermissive cells." In contrast, Vif is dispensable for replication in other T cells (e.g., SupT1), which are known as "permissive cells" (10, 36, 47). In early work on Vif, *vif*-deficient virions produced in nonpermissive cells were found to be significantly impaired in their ability to complete reverse transcription (12, 41, 47) as well as 100- to 1,000-fold less infectious than the wild type (WT) (8, 9, 43).

More recently, Sheehy et al. (38) identified APOBEC3G (APO3G), originally termed CEM15, as the cellular factor that restricts replication of *vif*-deficient HIV-1. APO3G expressed in nonpermissive cells is incorporated into *vif*-deficient virus particles, but its presence in WT virions is dramatically reduced (15, 20, 26, 27). In nonpermissive cells, Vif counteracts APO3G activity by targeting the inhibitor for degradation via the ubiquitination-proteosome pathway (5, 27, 28, 39, 42, 52), although other mechanisms may also be involved (20, 42).

APO3G is a member of a large family of cellular cytidine deaminases, which includes APOBEC1 (APO1) and activation-induced cytidine deaminase (AID) (19, 48). All of the APO proteins have one or two zinc finger domains containing the conserved motif (H/C)XE(X)$_{23\sim28}$CXXC (3, 48). APO3G has two zinc finger domains, which are important for the biochemical and biological activities of the protein. The APO enzymes catalyze deamination of cytosine residues in single-stranded DNA (ssDNA) and/or RNA to uracil. APO3G preferentially deaminates the terminal cytidine residue of the (T/C)CC sequence in ssDNA (2, 15, 24, 26, 44, 51, 54). This activity has the potential to greatly inhibit virus replication (6, 7, 11, 16, 21).

Until now, most of the studies on APO3G have been performed primarily in cell-based systems or with enzyme derived from virus lysates. To analyze the molecular properties of this protein and to investigate the mechanism of antiviral activity, we chose a more biochemical approach and set out to obtain highly purified, active enzyme. In earlier work it was reported that partially purified APO3G expressed in *Escherichia coli* has deaminase activity (15) (also see reference 2). However, at about the same time, another group was unable to detect this activity with a bacterially derived enzyme (54). Moreover, in our experience, we found that despite extensive efforts, purification of human APO3G expressed in *E. coli* failed to yield soluble, active protein, apparently because it does not fold properly (data not shown). Instead, we used a baculovirus expression system, and under these conditions we succeeded in producing enzymatically active glutathione *S*-transferase (GST)-tagged APO3G as well as untagged APO3G, which could each be purified to ~95%. Partially purified APO3G expressed as a GST fusion protein in baculovirus has been used in two previous studies (19, 44).

The availability of highly purified enzymatically active APO3G has made it possible for the first time to conduct a comprehensive molecular analysis of APO3G deamination and nucleic acid binding activities in the absence of other viral components that are present in viral lysates and without contaminating enzymes from the expression system. In this study, we show that while ssDNA is the exclusive substrate for deami-

* Corresponding author. Mailing address: Laboratory of Molecular Genetics, NICHD, Building 6B, Room 216, NIH, Bethesda, MD 20892-2780. Phone: (301) 496-1970. Fax: (301) 496-0243. E-mail: levinju@mail.nih.gov.

TABLE 1. Oligonucleotides used in this study

Name	Sequence[a]	Purpose
JL650	5′-p-GAT GAA GCC TCA CTT CAG AAA CAC AGT G-3′	Construction of pET-GST-APO3G WT
JL629	5′-CCA TGA CTC GAG TTA CTA GTT TTC CTG ATT CTG GAG AAT GGC-3′	Construction of pET-GST-APO3G WT
JL667	5′-AGC CCC TGC ACA AAG TCG ACA AGG GAT ATG-3′	Construction of C100S mutation
JL668	5′-CAT ATC CCT TGT CGA CTT TGT GCA GGG GCT-3′	Construction of C100S mutation
JL648	5′-AGC CCC TGC TTC AGC AGT GCA CAG GAA ATG GCT-3′	Construction of C291S mutation
JL649	5′-AGC CAT TTC CTG TGC ACT GCT GAA GCA GGG GCT-3′	Construction of C291S mutation
JL82	5′-AAA AGA AAA GGG GGG ACT GG-3′	Deamination assay
JL186	5′-AGT GAA TTA GCC CTT CCA GTC CCC CCT TTT CTT TT-3′	Deamination assay
JL194	5′-aaa aga aaa ggg ggg acu gg-3′	Deamination assay
JL651	5′-ATT ATT ATT ATT ATT ATT ATT CUG CGG ATT TAT TTA TTT A-3′	Deamination assay
JL653	5′-ATT ATT ATT ATT ATT ATT ATT CCC AGG ATT TAT TTA TTT A-3′	Deamination assay
JL665	5′-TAA ATA AAT AAA TCC-3′	Deamination assay
JL699	5′-auu auu auu auu auu auu auu ccc agg auu uau uua uuu a-3′	Deamination assay
JL700	5′-ATT ATT ATT ATT ATT ATT ATT C(mC)(mC) AGG ATT TAT TTA TTT A-3′	Deamination assay
JL640	5′-ATT ATT ATT ATT ATT ATT ATT CCG CGG ATT TAT TTA TTT A-3′	Deamination assay and EMSA
JL641	5′-ATA AAT CCG CGG AAT AAT-3′	EMSA
JL652	5′-TAA ATA AAT AAA TCC GCG GAA TAA TAA TAA TAA TAA TAA T-3′	EMSA
JL654	5′-auu auu auu auu auu auu auu ccg cgg auu uau uua uuu a-3′	EMSA
JL655	5′-uaa aua aau aaa ucc gcg gaa uaa uaa uaa uaa uaa uaa u-3′	EMSA
JL657	5′-AAA AAA AAA AAA AAA AAA AAA AAA AAA AAA AAA AAA A-3′	EMSA
JL658	5′-TTT TTT TTT TTT TTT TTT TTT TTT TTT TTT TTT TTT T-3′	EMSA
JL659	5′-CCC CCC CCC CCC CCC CCC CCC CCC CCC CCC CCC CCC C-3′	EMSA
JL660	5′-UUU UUU UUU UUU UUU UUU UUU UUU UUU UUU UUU UUU U-3′	EMSA
JL670	5′-TAT TAT TAT TAT TCC GCG GAT TTA-3′	EMSA
JL671	5′-TTA TTA TTC CGC GGA TTT ATT T-3′	EMSA
JL672	5′-TAT TAT TCC GCG GAT TTA TT-3′	EMSA
JL673	5′-TTA TTC CGC GGA TTT A-3′	EMSA
JL674	5′-TAT TCC GCG GAT TT-3′	EMSA
JL765	5′-aaa aau uuu gac uag cgg agg cua gaa gga gag-3′	EMSA

[a] Uppercase and lowercase denote deoxyribo- and ribonucleotides, respectively. Note that the uppercase U is a deoxyuridine. The "p" and "(mC)" represent monophosphorylated modification at the 5′ end and 5-methyldeoxycytidine, respectively.

nation, APO3G binds efficiently to both ssDNA and ssRNA, approximately half as well to a DNA/RNA hybrid, and poorly to double-stranded DNA (dsDNA) and dsRNA. We also report that the nucleotide specificities for deamination and binding of ssDNA are not correlated. Finally, using purified wild-type (WT) and zinc finger mutant proteins, we demonstrate that the two zinc finger domains play differing roles with respect to nucleic acid binding, deamination, and antiviral activity and speculate on the implications of our findings for the mechanism of the antiviral effect.

MATERIALS AND METHODS

Oligonucleotides. Oligonucleotides (oligos) used in this study were purchased from Integrated DNA Technologies or Lofstrand and are listed in Table 1 according to their use in particular experiments. For electrophoretic mobility shift assays (EMSAs) and deamination assays, DNA and RNA oligos were first gel purified by denaturing polyacrylamide gel electrophoresis (PAGE). Where indicated, oligos were 5′ end labeled with [γ-^{32}P]ATP (3,000 Ci/mmol) (GE Healthcare) using T4 polynucleotide kinase (Ambion), as described previously (13).

Plasmid construction. To construct a plasmid for APO3G expression in a baculovirus system, a DNA fragment of the complete APO3G open reading frame was amplified by PCR from pcDNA-APO3G (20), using primers JL650 and JL629, and was then inserted into the pET41a(+) vector (Novagen) between the PshAI and XhoI restriction sites. The resulting plasmid is called pET-GST-APO3G-WT. An XbaI and XhoI fragment was cloned into pFastBac1 (Invitrogen) and named pFastBac-GST-APO3G-WT. For construction of zinc finger mutants with a Cys-to-Ser change, two DNA fragments, each with a single mutation, were made by PCR using the following primers: for C100S, JL667 and JL668; for C291S, JL648 and JL649. The DNA fragments were inserted into pFastBac-GST-APO3G-WT between AflII and XhoI. To create a double zinc finger mutant, two DNA fragments, AflII-BamHI with the C100S mutation and BamHI-XhoI having the C291S mutation, were inserted into pFastBac-GST-APO3G-WT between AflII and XhoI. For expression of APO3G in HeLa cells, the DNA fragments (AflII-XhoI) of pFastBac-GST-APO3G-C100S, pFastBac-GST-APO3G-C291S, and pFastBac-GST-APO3G-C100S/C291S were inserted into the pcDNA-APO3G-WT previously cut with AflII and XhoI. In all cases, the sequences of both the insert and the boundary regions were verified by DNA sequencing by the University of Maryland Biopolymers Laboratory.

Purification of human APO3G and mutant proteins. The pFastBac-GST-APO3G plasmids, containing either WT or zinc finger mutations, were used to make recombinant bacmid DNA in *E. coli* DH10Bac, according to the protocol supplied by the manufacturer for the Bac-to-Bac Baculovirus Expression System (Invitrogen). To obtain recombinant viruses, Sf21 cells were transfected with each bacmid DNA by using Cellfectin (Invitrogen); high-titer viruses were isolated. For expression of GST-APO3G proteins, Sf21 cells were infected at a multiplicity of infection of 1, incubated for 72 h at 27°C, and then collected by centrifugation.

The cells were disrupted by sonication in lysis buffer (25 mM HEPES [pH 7.0], 500 mM NaCl, 1% Triton X-100, 10 mM $CaCl_2$, 1 mM EDTA, 5 mM 2-mercaptoethanol [2-ME], 10% glycerol, 1 mM phenylmethylsulfonyl fluoride, complete protease inhibitor [Roche]). DNase I (5 U/ml) and RNase A (40 μg/ml) were added, and the entire mixture was kept on ice for 1 h. The soluble fraction was isolated by centrifugation at 20,000 $\times$ *g* for 30 min and was bound to glutathione Sepharose High Performance resin (GE Health Care) for 3 h at 4°C. To facilitate dissociation of residual nucleic acids from the protein, the resin was first washed with lysis buffer containing 1 M NaCl without glycerol or protease inhibitors and then with lysis buffer containing 500 mM NaCl without protease inhibitors. The bound GST-APO3G proteins were eluted with glutathione buffer (50 mM Tris-HCl [pH 7.4], 10 mM NaCl, 40 mM reduced glutathione, 5% glycerol, 10 μM $ZnCl_2$), and the eluate was dialyzed against Enterokinase buffer (Novagen). To obtain APO3G without a GST tag, the dialyzed solution was diluted (so that the APO3G concentration was about 10 μM) and then incubated in the presence of recombinant Enterokinase (5 U/ml) (Novagen) at 21°C for 12 h. Although most of the cleaved APO3G was precipitated, only the soluble fraction (approximately 10 to 30% of the total protein) was collected for the next step. In contrast to APO3G, GST-tagged APO3G proteins remained highly

soluble. APO3G and the GST-tagged proteins were subjected to fractionation on a high-performance liquid chromatography-DEAE column (10 μm; 75 by 7.5 mm; Tosoh Bioscience), using a linear gradient from 20 to 1,000 mM of NaCl with a flow rate of 1 ml/min over 50 min. The solutions used to make the gradient were Buffer A (50 mM Tris-HCl [pH 7.4], 20 mM NaCl, 10% glycerol, 0.5% Triton X-100, 1 mM 2-ME) and Buffer B, which is identical to Buffer A except that the NaCl concentration is 1,000 mM. APO3G was eluted after ~21 min. Protein concentrations were determined using a Coomassie Plus kit (Pierce). Note that the legends specify whether untagged APO3G (referred to as "APO3G") or tagged APO3G (referred to as "GST-APO3G") was used in a particular experiment.

Cytidine deamination assays. Two different methods were used to detect deaminase activity of APO3G: (i) a UDG-dependent assay and (ii) primer extension terminated with a dideoxynucleotide.

(i) UDG-dependent assay. The ^{32}P-labeled substrate (30 nM) was incubated in deamination buffer (10 mM Tris-HCl [pH 8.0], 50 mM NaCl, 1 mM EDTA, 1 mM dithiothreitol [DTT]) at 37°C for 90 min in the presence or absence of APO3G (or GST-APO3G) (0.4 to 1.2 μM). UDG from *E. coli* (2 U) (New England Biolabs) and UDG buffer were added to the deamination reaction mixture, which was incubated at 37°C for 45 min. The reaction mixture was treated with 0.15 M NaOH at 37°C for 20 min, heated at 95°C for 5 min, and then promptly chilled on ice. After separation of the cleavage products by PAGE in a 15% denaturating gel, the radioactivity in the gel was quantified by scanning with a PhosphorImager (GE Healthcare) in the linear range of band intensity, followed by analysis with ImageQuant software.

(ii) Primer extension terminated with a dideoxynucleotide. As described above for the UDG-dependent protocol, the substrate (30 nM) was incubated in deaminase buffer at 37°C for 90 min in the presence or absence of GST-APO3G (1.2 μM). The deaminated substrate was annealed to a ^{32}P 5′-end-labeled primer (45 nM) (JL665) by heating at 85°C for 5 min and then gradually cooling to 25°C. An equal volume of primer extension cocktail (100 mM Tris-HCl [pH 8.0], 150 mM KCl, 14 mM $MgCl_2$, 2 mM DTT, 1.0 U/μl of SUPERaseIn [Ambion]), 20 nM HIV-1 reverse transcriptase (RT) (Worthington), 100 μM dideoxy ATP, and 100 μM each of dTTP and dGTP was added to the annealed product, and the mixture was incubated at 37°C for 15 min. Reactions were terminated by freezing on dry ice, followed by addition of gel loading buffer II (Ambion). The products were separated by PAGE in a 15% denaturing gel. Radioactivity was quantified as described above.

Electrophoretic mobility shift assays (EMSAs) with APO3G. For formation of a duplex, the labeled oligo was heat annealed to its complement at a ratio of unlabeled to labeled oligo of 1.5:1. The labeled oligo (30 nM) was incubated with the indicated concentration of purified proteins in gel-shift reaction buffer (50 mM Tris-HCl [pH 8.0], 75 mM KCl, 7 mM $MgCl_2$, 1 mM DTT) at 37°C for 15 min. The resulting complexes were separated in native gels (4 or 6%) at 4°C. Radioactivity in the gel was quantified as described above. The percentage of substrate that was shifted (% Shifted) was calculated by dividing the volume of the shifted bands by the total volume of each lane and then multiplying by 100.

Dissociation constant values (K_D) were estimated by plotting binding activity versus concentration of APO3G from EMSA results with a 20-nucleotide (nt) ssDNA, since essentially one shifted band is formed in this case. Briefly, the K_D is defined as [A][P]/[A · P], where A is the APO3G protein, P is the oligo, and A · P is the APO3G-oligo complex. The total oligo concentration (PT) is defined as [PT] = [P] + [A · P]. If the ratio of shifted bands, B, is defined as B = [A · P]/[PT], then by manipulating the dissociation constant equations K_D can be calculated as follows: $K_D = [A](1/B - 1)$.

The HIV-1 nucleocapsid protein (NC) used in this work was the generous gift of Robert J. Gorelick (SAIC-Frederick, Inc., Frederick, Md). The protein was prepared as described previously (50).

Virus production and analysis of virus infectivity. Virus production and analysis of virus infectivity were performed as reported previously (46). Briefly, to obtain virus particles, APO3G-negative HeLa cells were cotransfected with the *vif*-defective full-length molecular clone HIV-1 pNL4-3*vif*(−) and pcDNA APO3G or pcDNA 3.1 (vector control). Virus infectivity was determined by single-cycle replication assays with LuSIV cells, obtained from the AIDS Research and Reference Reagent Program, National Institute of Allergy and Infectious Diseases, National Institutes of Health (catalog no. 5460; cells were originally obtained from J. W. Roos and J. E. Clements) (34). Infectivity was calculated by normalizing for the amount of input RT activity.

Incorporation of APO3G into virions. For immunoblot analysis of APO3G present in the cell and in virions, the following procedure was used. Cells were washed once with phosphate-buffered saline (PBS), suspended in PBS (200 μl per 5×10^6 cells), and then mixed with an equal volume of 2× Laemmli buffer (Bio-Rad) containing 5% 2-ME. To prepare virus-associated proteins, cell-free-filtered supernatants from transfected HeLa cells (7 ml) were pelleted (75 min, 151,000 × *g*) through a 20% sucrose cushion (4 ml) in an SW41 rotor. The concentrated virus pellet was suspended in PBS (50 μl) and was mixed with an equal volume of 2× Laemmli buffer. Proteins were solubilized by heating for 10 to 15 min at 95°C. Cell lysates were normalized according to cell number, and virus lysates were normalized according to RT activity. Samples were subjected to sodium dodecyl sulfate (SDS)-PAGE; proteins were transferred to polyvinylidene difluoride membranes and reacted with anti-APO3G rabbit serum (20). To detect capsid (CA) protein, anti-CA rabbit serum (obtained from the AIDS Research and Reference Reagent Program, National Institute of Allergy and Infectious Diseases, National Institutes of Health; catalog no. 4250) was used. The membranes were then incubated with alkaline phosphatase-conjugated secondary antibodies (Applied Biosystems), and the proteins were visualized by the Western-Star system (Applied Biosystems).

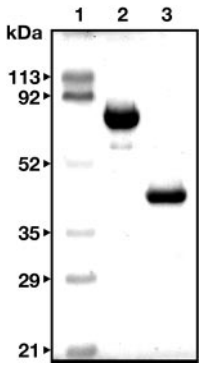

FIG. 1. Purification of APO3G from a baculovirus expression system. Purified GST-APO3G and APO3G proteins were resolved by electrophoresis in an SDS–10% polyacrylamide gel and stained with Coomassie brilliant blue R-250. Lanes: 1, prestained SDS-PAGE standard (low range) molecular marker (Bio-Rad); 2, 5 μg of GST-APO3G; and 3, 3 μg of APO3G. Approximate molecular sizes are indicated on the left.

RESULTS

Enzymatic properties of purified APO3G expressed in a baculovirus system. To perform a detailed analysis of the biochemical properties of APO3G, the protein was expressed with an N-terminal GST tag in a baculovirus system and purified. Figure 1 shows the migration of purified GST-APO3G (~78 kDa) in an SDS–10% polyacrylamide gel (lane 2). Since the protein solubility is low, APO3G precipitated once the tag was removed. However, there was still sufficient soluble protein to allow further purification (lane 3). Based on Coomassie staining of the gel, the purity of APO3G (~46 kDa) (lane 3) and GST-tagged APO3G (lane 2) was estimated to be ~95%.

The cytidine deaminase activity of APO3G was tested using a UDG-dependent assay. To determine substrate specificity, we prepared ssDNA, dsDNA, and a DNA/RNA hybrid, each containing the same minus-strand DNA sequences (Fig. 2A). There are three regions containing potential deamination sites, which we designated regions I, II, and III (Fig. 2A). In the absence of HIV-1 NC (Fig. 2B), APO3G deaminated cytidines in all three of these regions in ssDNA (lane 4). This indicates that both CCC and TCC represent deamination motifs recognized by APO3G, in agreement with earlier results (15, 24, 26, 44, 51, 54). No deamination was detected in the absence of APO3G (lanes 1 to 3).

In contrast to the results with ssDNA, DNAs annealed to a complementary 20-nt DNA (lane 5) or RNA (lane 6) could not

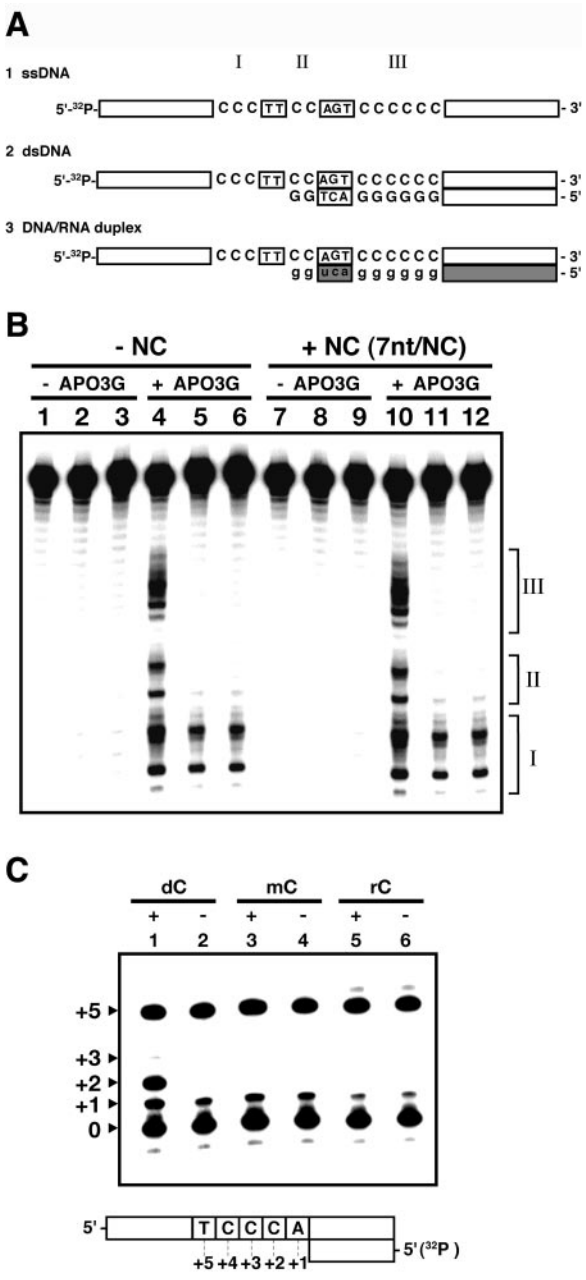

FIG. 2. Substrate specificity for deamination by purified APO3G or GST-APO3G. (A) Substrates for the UDG-dependent deamination assay were the following: 1, 35-nt ssDNA oligonucleotide (JL186); 2, JL186 annealed to a 20-nt DNA (JL82); or 3, to a 20-nt RNA (JL194). In each case, the ssDNA was labeled at its 5′ end with ^{32}P. The sites where deamination can occur (at CCC and TCC sequences) are divided into three regions: I, II, and III. The flanking sequences are not shown. (B) The deaminase activity of purified APO3G (1.0 μM) was determined by the UDG-dependent assay in the presence or absence of NC (7 nt/NC). The substrates were the following: 35-nt ssDNA oligo (JL186) (lanes 1, 4, 7, and 10), JL186 annealed to a 20-nt DNA (JL82) (lanes 2, 5, 8, and 11), or JL186 annealed to a 20-nt RNA (JL194) (lanes 3, 6, 9, and 12). (C) Deamination of ssDNA, containing dC or mC residues at positions 2 and 3, and ssRNA was measured by using the primer extension assay. The substrates were incubated with (+) or without (−) GST-APO3G (1.2 μM) at 37°C for 90 min. Following annealing of the ^{32}P-labeled primer (JL665) to the deaminated substrates, the primer was extended by HIV-1 RT in the presence of ddATP (plus dTTP and dGTP). The numbers on the left show how many bases were extended from the primer. The substrates "dC", "mC", and "rC" refer to DNA oligos JL653 and JL700 and RNA oligo JL699, respectively.

be deaminated in region II or III, which forms a dsDNA or a DNA/RNA hybrid, respectively. However, the dCs in single-stranded region I were deaminated, forming the same region I products as ssDNA. These results demonstrate that purified APO3G has single-strand-specific DNA deaminase activity. Although HIV-1 NC is a required cofactor for reverse transcription (25), the deamination pattern and efficiency of APO3G with these substrates were unaffected by the presence of NC (lanes 10 to 12). This suggests that NC does not interfere with the deamination activity of APO3G. The results also imply that ssDNA remains a target for APO3G even when the DNA is bound to NC.

Since the cytidine residue in the CpG sequence is frequently methylated in the eukaryote genome (33), it was also of interest to determine whether APO3G can deaminate dC with a methyl group at position 5, i.e., 5-methyldeoxycytidine (5mC). For this purpose, we developed an alternative deaminase assay in which primer extension is terminated by a dideoxynucleotide. We devised this assay because the putative deamination product of 5mC is thymidine, which is not a substrate for UDG.

Figure 2C demonstrates that in reactions containing the dC sample (positive control), the dideoxy ATP (ddATP) mixture, and GST-APO3G, a strong +2 band was generated in addition to a +5 product (lane 1). This indicates that deamination of dC to dU occurred predominantly at position 2. The appearance of a +5 product shows that a portion of the substrate was not deaminated, and therefore some extension could continue until the T residue at position 5 (lane 1). The +1 band appeared in the presence or absence of APO3G and is likely to be a pause product (lanes 1 and 2). In the absence of GST-APO3G, the predominant product was a +5 band (lane 2). In contrast, with the methylated substrate a +5 band was the major product detected in either the presence or absence of APO3G; the +1 pause product was also observed (lanes 3 and 4). Thus, there was no evidence for deamination of 5mC residues. The same conclusion was reached when the experiment was repeated with a dideoxy GTP (ddGTP) mixture (with dTTP and dATP) (data not shown).

Additionally, we found that methylation blocked deamination of an ssDNA containing the sequence TC(5mC)G (data not shown). Thus, if single-stranded regions of genomic DNA containing methylated CpG were to come in contact with APO3G, these DNA regions would be protected from APO3G deaminase activity.

We also investigated whether cytosines in ssRNA can be deaminated by APO3G (Fig. 2C). Since UDG does not react with uracils in RNA, our approach was to use the primer extension assay to address this question. As observed with the mC substrate, a +2 termination product could not be detected with the ddATP mixture in the presence (lane 5) or absence (lane 6) of APO3G. Taken together, these results indicate that APO3G cannot significantly deaminate ssRNA in this system.

Characteristics of APO3G binding to nucleic acids. Detailed analysis of APO3G nucleic acid binding activity has not been

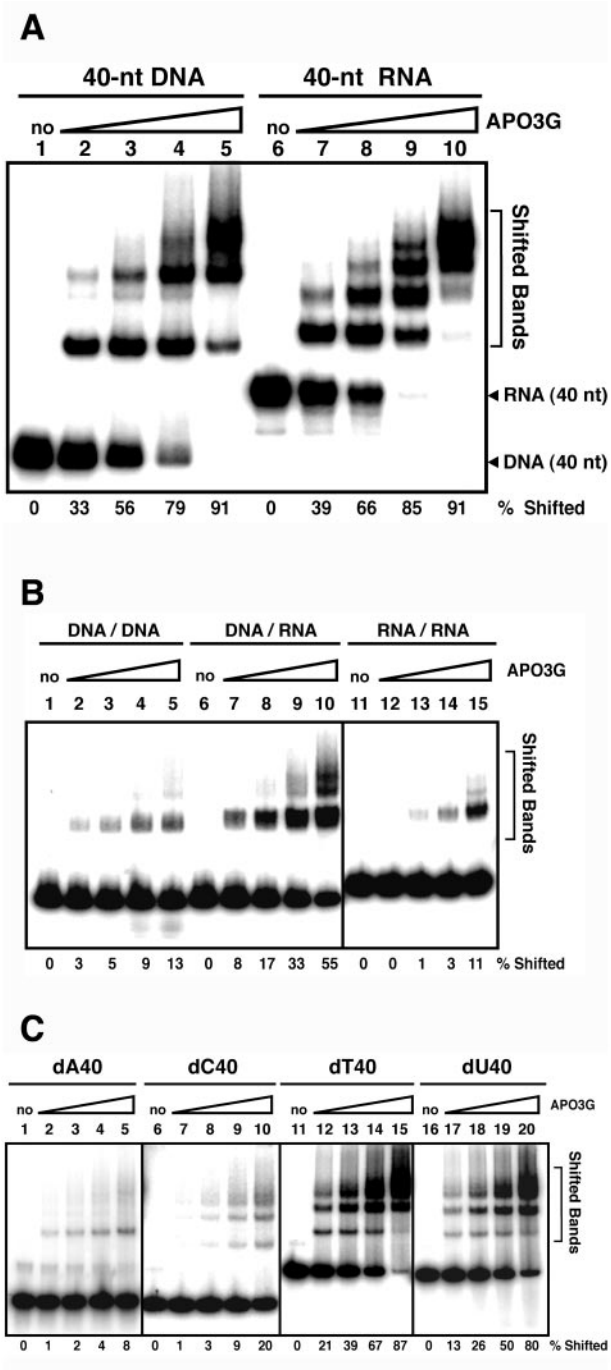

FIG. 3. Nucleic acid binding properties of APO3G analyzed by EMSA. In all of the gels, the values for "% Shifted" (%) were calculated as described in the text. (A) The binding affinities of APO3G for ssDNA (JL640) and ssRNA (JL654) were determined by EMSA. Forty-nucleotide DNA and RNA oligos having the same sequence were used. The APO3G concentrations were the following: lanes 1 and 6, 0 nM; lanes 2 and 7, 20 nM; lanes 3 and 8, 40 nM; lanes 4 and 9, 80 nM; and lanes 5 and 10, 160 nM. (B) The binding affinity of APO3G for double-stranded oligos was tested with dsDNA (JL640/JL652), a DNA/RNA hybrid (JL640/JL655), and dsRNA (JL654/JL655). One oligo in each pair was radiolabeled: JL640 and JL654. The APO3G concentrations for each set (lanes 1 to 5, 6 to 10, and 11 to 15) were the same as the concentrations given for lanes 1 to 5 in the legend to panel A. (C) The sequence specificity of APO3G binding was investigated with the following 40-nt homopolymeric DNAs: dA40, JL657; dC40, JL659; dT40, JL658; and dU40, JL660. The APO3G concentrations for each set (lanes 1 to 5, 6 to 10, 11 to 15, and 16 to 20) were the same as the concentrations given for lanes 1 to 5 in the legend to Fig. 3A. In this figure as well as in succeeding figures, gel images from EMSA reactions run on the same gel are enclosed within a box.

reported thus far. Using purified APO3G, we initially compared the binding affinity of APO3G to DNA and RNA by EMSA. As shown in Fig. 3A, as the concentration of APO3G was raised an increase in the number of high-molecular-weight complexes and a greater proportion of shifted material could be detected; at the highest concentration, the percent shifted value reached 91% for both the RNA and DNA samples. A slightly higher amount of shifted bands was observed with the 40-nt RNA compared with the 40-nt DNA at lower APO3G concentrations. However, these differences were small, suggesting that the binding affinities of APO3G to RNA and DNA were actually quite similar. Note that in each case, with high concentrations of APO3G, four shifted bands with different mobilities could be detected. We assume that these bands represent four different nucleic acid-APO3G complexes. Interestingly, in other EMSA experiments, APO3G bound with similar efficiency to 33-nt DNA or RNA oligos containing the biologically relevant HIV-1 SL-3 stem-loop sequence, which in the RNA form represents the major viral RNA packaging signal and is located at the 5′ end of the genome (35) (data not shown).

To determine whether binding is specific for single-stranded nucleic acids, EMSA was also performed with dsDNA, a DNA/RNA hybrid, and dsRNA (Fig. 3B). These oligos had the same DNA or RNA sequence as those used in Fig. 3A, in addition to the appropriate 40-nt complement. The results showed that at the highest concentration of APO3G (160 nM), the protein bound approximately four- to fivefold more efficiently to the DNA/RNA hybrid (55% shifted) (lane 10) than to either dsDNA (lane 5) or dsRNA (lane 15) (13% and 11% shifted, respectively). These data indicate that although APO3G binding to the DNA/RNA hybrid was significant, it was still approximately twofold lower than that observed with ssRNA or ssDNA at comparable concentrations of APO3G (compare Fig. 3A with B).

We also examined the nucleotide preference for APO3G binding using 40-nt homopolymeric DNA oligos (Fig. 3C). The data indicated that APO3G could bind efficiently to dT40 or dU40 (lanes 15 and 20, 87% and 80% shifted, respectively, at the highest APO3G concentrations) but with less efficiency to dC40 (lane 10, 20% shifted) and dA40 (lane 5, <10% shifted). (Note that we were unable to analyze dG40 because of its low solubility.) Surprisingly, these results indicated that the nucleotide preferences for APO3G binding (dT or dU) differ from the requirement for dC-containing motifs for deamination (Fig. 2B). It is also of interest that at the highest APO3G concentration, four different shifted bands were observed, as in Fig. 3A. This finding demonstrates that the number of shifted bands is independent of the oligo sequence.

The data of Fig. 3 showing formation of a greater number of higher order complexes with increasing APO3G concentrations also suggest the possibility that when APO3G binds, it

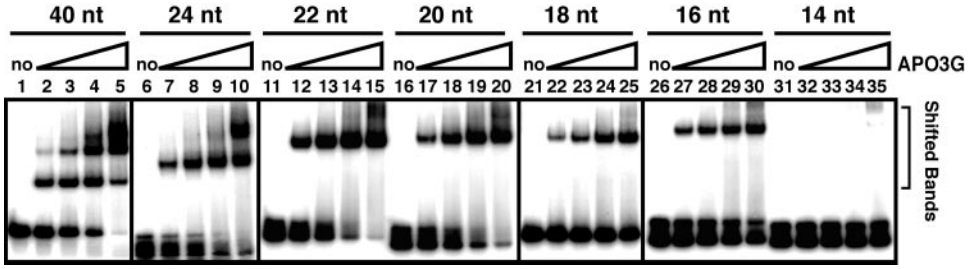

FIG. 4. Minimum length required for APO3G binding to ssDNA. The length and designation of each oligo were the following: 40 nt, JL640; 24 nt, JL670; 22 nt, JL671; 20 nt, JL672; 18 nt, JL641; 16 nt, JL673; and 14 nt, JL674. The APO3G concentrations (lanes 1 to 5, 6 to 10, 11 to 15, 16 to 20, 21 to 25, 26 to 30, and 31 to 35) were the same as the concentrations given for lanes 1 to 5 in the legend to Fig. 3A.

covers a certain length of nucleic acid. To investigate the relationship between nucleotide length and APO3G binding, we measured binding to DNA oligos ranging in size from 14 to 40 nt (Fig. 4). When 24- and 22-nt DNAs were used, two shifted bands were detected with high concentrations of APO3G (lanes 9 and 10 and lanes 14 and 15, respectively), although the intensity of the uppermost band formed with the 22-nt DNA was significantly reduced compared with the analogous band seen with the 24-nt DNA. With the 20-, 18-, or 16-nt DNAs (lanes 19 and 20, 24 and 25, and 29 and 30, respectively), there was essentially only one shifted band. In contrast, a distinct shifted band could not be observed with the 14-nt DNA (lanes 32 to 35). These results demonstrate that APO3G binds nucleic acids that are 16 nt or greater in length.

It seems reasonable to assume that when there is only a single shifted band, it may consist of a single uniform nucleic acid-APO3G complex. Using data from EMSAs with the 20-nt DNA, the K_D value for binding was estimated to be $\sim 76 \pm 21$ nM. To exclude the possibility that the results showing a minimum binding length of 16 nt might be affected by sequence preference, we also tested the binding affinity of APO3G to 16- and 14-nt ssDNAs consisting of repeated sequences of either dTA or dCA. In accord with the observations in Fig. 4, we found that with both sets of oligos, a length of 16 nt was critical for significant APO3G binding (data not shown).

RNA binding in the presence of APO3G and HIV-1 NC. To assess the effect of HIV-1 NC on APO3G binding to nucleic acid, EMSA was performed with increasing concentrations of APO3G (0 to 160 nM) in the presence of a constant amount of NC (Fig. 5A). The NC level was set at 7 nt/NC, which is within the range of the binding site size calculated from in vitro experiments (25) and is also in agreement with the estimated ratio of nucleotides to NC molecules in the virion (17). Since NC did not bind efficiently to relatively small ssRNA oligos (e.g., 18 nt) (data not shown), we performed these studies with a 40-nt ssRNA (JL654, an AU-rich RNA oligo that does not form a secondary structure). The 40-nt ssRNA was preincubated with NC prior to addition of APO3G. In reactions with NC and APO3G (lanes 7 to 10), the RNA bands migrated more slowly than in the absence of NC and the presence of APO3G (lanes 2 to 5). (Note that the same effect of NC was observed even if APO3G was omitted [compare lanes 1 and 6].) These results suggest that when APO3G and NC were both present in the reaction, the shifted bands represented a complex with RNA, NC, and APO3G. In addition, the data show that NC did not interfere with APO3G binding to ssRNA.

In Fig. 5B, the reverse experiment was performed, i.e., a fixed amount of APO3G was bound to the RNA before addition of increasing amounts of NC (up to 1.75 nt/NC). At a given concentration of APO3G (20 or 80 nM), the relative amounts of bands shifted by APO3G were independent of NC concentration (lanes 6 to 15). Moreover, as seen in Fig. 5A, when NC and APO3G were both present in the reaction, the RNA bands were "super" shifted. This was especially evident with 80 nM APO3G (lanes 11 to 15). These results indicate that APO3G did not affect NC binding to the RNA oligo.

Interestingly, when the 33-nt SL-3 RNA sequence was used in the same assay, somewhat different results were obtained. In Fig. 5C, NC was bound to the RNA prior to addition of APO3G (lanes 6 to 10). As may be seen, SL-3 RNA was shifted more efficiently in reactions containing NC compared to reactions without NC (compare lanes 7 to 10 with lanes 2 to 5). This effect was most noticeable at the highest APO3G concentrations (compare lanes 9 and 10 with lanes 4 and 5). A similar phenomenon was observed with reactions in which the RNA was preincubated with APO3G before addition of NC (Fig. 5D). Thus, when fixed concentrations of APO3G and increasing concentrations of NC were added (lanes 7 to 10 and 12 to 15), there was a corresponding increase in the amount of the slowest migrating band. The increased binding efficiency was particularly striking when the pattern of shifted bands was compared at the 160 nM concentration of APO3G (lanes 11 to 15). In this case, the faster migrating bands seen in the reaction without NC (lane 11) were almost completely absent in the reactions with the highest concentrations of NC (lanes 14 and 15). The results with SL-3 RNA also suggest that the shifted bands contained both NC and APO3G.

Taken together, the data in Fig. 5 demonstrate that HIV-1 NC and APO3G do not interfere with each other's binding to RNA and in fact form a complex containing RNA and both proteins. In addition, with SL-3 RNA, binding efficiency of APO3G was augmented when NC was present (see below).

Roles of the zinc finger domains in APO3G nucleic acid binding in vitro and its incorporation into virus particles. To assess the contribution of the zinc finger domains to the nucleic acid binding activity of APO3G, we first performed an EMSA in which APO3G was bound to ssDNA in the presence of the zinc chelating agent 1,10 phenanthroline. The results showed that zinc coordination is essential for APO3G binding to nucleic acids (data not shown). To investigate the function of each individual domain, we purified GST-APO3G containing the following zinc finger mutations with a Cys-to-Ser change:

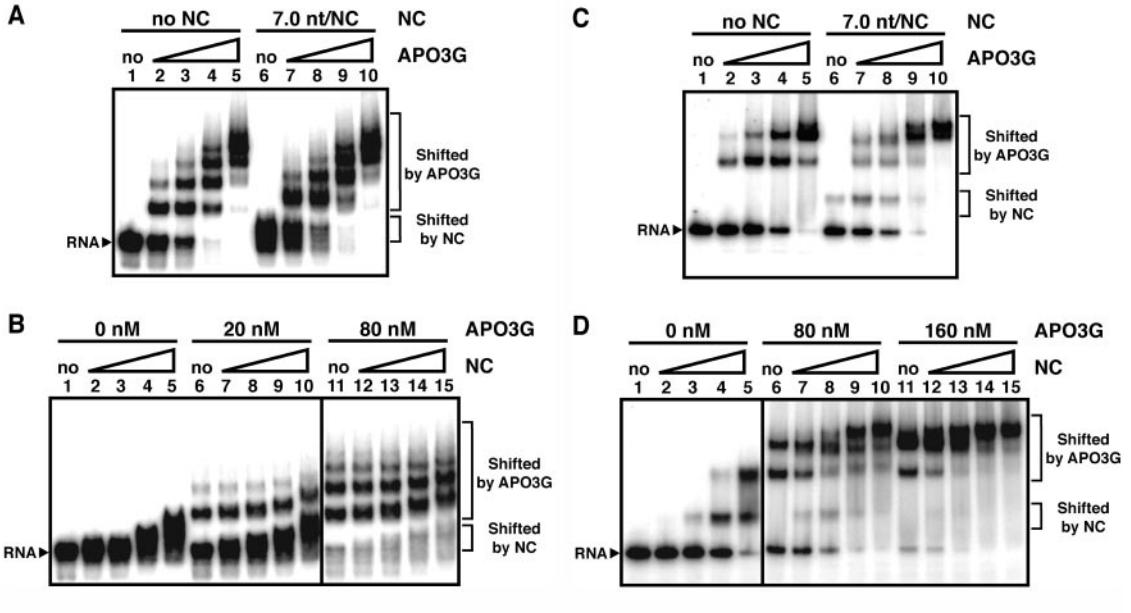

FIG. 5. RNA binding of APO3G or HIV-1 NC in the presence of HIV-1 NC or APO3G, respectively. The EMSAs were performed with a 40-nt ssRNA (JL654) or a 33-nt SL-3 RNA (JL765). (A and C) The RNA (JL654 [A] or JL765 [C]) was preincubated for 15 min at 37°C without (lanes 1 to 5) or with NC (equivalent to 7 nt/NC) (lanes 6 to 10), prior to addition of APO3G. The following concentrations of APO3G were then added to the NC-RNA complex: no APO3G, lanes 1 and 6; 20 nM, lanes 2 and 7; 40 nM, lanes 3 and 8; 80 nM, lanes 4 and 9; 160 nM, lanes 5 and 10. (B) The same procedure was followed, except that APO3G at 0 nM (lanes 1 to 5), 20 nM (lanes 6 to 10), or 80 nM (lanes 11 to 15) was preincubated with the RNA prior to addition of NC. The NC concentrations were the following: lanes 1, 6, and 11, no NC; lanes 2, 7, and 12, 14 nt/NC; lanes 3, 8, and 13, 7 nt/NC; lanes 4, 9, and 14, 3.5 nt/NC; and lanes 5, 10, and 15, 1.75 nt/NC. (D) The procedure described for panel B was followed, except that APO3G at a concentration of 0 nM (lanes 1 to 5), 80 nM (lanes 6 to 10), or 160 nM (lanes 11 to 15) was preincubated with SL-3 RNA prior to addition of NC. The NC concentrations were the same as those in panel B.

first domain, C100S; second domain, C291S; and a double mutant, C100S/C291S.

The binding affinities at increasing protein concentrations of wild-type (WT) GST-APO3G and the three mutants were analyzed by EMSA (Fig. 6A) using a 40-nt ssDNA. The results showed that although the values for percentage of ssDNA shifted with WT (lanes 2 to 5) or C291S (lanes 12 to 15) were similar, at comparable concentrations binding activity of C100S (lanes 7 to 10) was reduced by approximately twofold. A drastic loss of binding activity was observed with the double mutant, C100S/C291S (lanes 17 to 20). Similar findings were made in EMSAs with a 20-nt ssDNA, and the K_D values were estimated as follows: WT, ~140 nM; C100S, ~320 nM; C291S, ~130 nM; and C100S/291S, ~55 μM. Note that the WT K_D value for GST-APO3G was similar (approximately twofold higher) to that obtained for untagged APO3G with a 20-nt ssDNA (~76 nM). Taken together, these findings indicate that both zinc fingers have the capacity to bind nucleic acid, illustrating the redundancy in zinc finger function with respect to binding. However, the contribution of the first zinc finger domain is more significant than that of the second domain.

To determine whether the binding capacity of APO3G WT and zinc finger mutants is correlated with the ability to encapsidate APO3G, we analyzed the effect of the zinc finger mutations on the incorporation of the protein into virions (Fig. 6B). Cellular expression levels of C100S (lane 2), C291S (lane 3), and C100S/291S (lane 4) were slightly less (74%, 80%, and 74%, respectively) than the WT level (set at 100%) (lane 1). The amounts of protein incorporated into virions were similar for the WT (lane 1) and C291S mutant (83% of WT) (lane 3), but encapsidation by the C100S mutant was approximately 55% of the WT level (lane 2). In contrast, the double mutation essentially eliminated incorporation of APO3G into virus particles (4% of WT) (lane 4). These data mirror the results shown in Fig. 6A. Note that the zinc finger mutations did not affect virus production, since each sample contained the same amount of CA (Fig. 6B, lowest panel).

Thus, taken together, the results of Fig. 6 demonstrate that the level of encapsidation of APO3G into virions (Fig. 6B) is correlated with the nucleic acid binding affinity measured in vitro (Fig. 6A). Moreover, although both zinc fingers have binding and encapsidation capabilities, the first zinc finger domain plays a more important role than the second zinc finger domain.

Correlation between deaminase activity and the anti-HIV-1 effect of APO3G. To clarify the effect of the zinc finger mutations on deaminase activity, we measured the activity of the purified WT and zinc finger mutant GST-APO3G proteins directly, using the UDG assay. As shown in Fig. 7A, WT and C100S had very similar levels of activity (lanes 1 and 2, respectively), whereas C291S and the double mutant had no detectable activity (lanes 3 and 4, respectively). The positive control shown in lane 6 was a dU-containing substrate, treated only with UDG. Note that some of the original material remained at the origin, indicating that UDG treatment was not com-

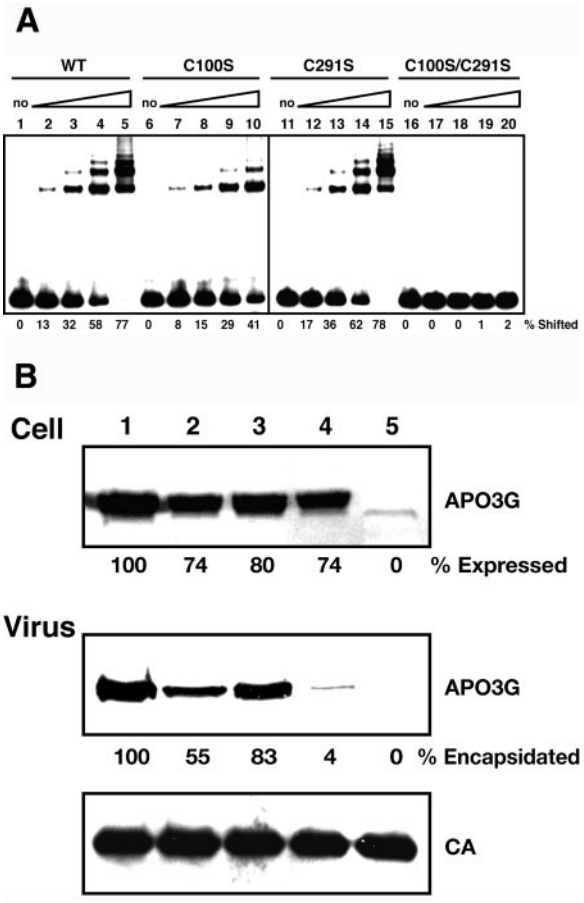

FIG. 6. Zinc finger-dependent nucleic acid binding affinity of APO3G and its relation to encapsidation of APO3G. (A) Nucleic acid binding activity was examined with purified GST-APO3G proteins. WT GST-APO3G as well as three zinc finger mutants, C100S, C291S, and C100S/C291S, were tested by EMSA performed with a 40-nt ssDNA (JL640). The following concentrations of each protein were used for the reactions: lane 1, 6, 11, and 16, 0 nM; lanes 2, 7, 12, and 17, 33 nM; lanes 3, 8, 13, and 18, 65 nM; lanes 4, 9, 14, and 19, 130 nM; and lanes 5, 10, 15, and 20, 260 nM. (B) Incorporation of APO3G WT and zinc finger mutant proteins into HIV-1 virions was examined by Western blot. Cell lysates were normalized according to cell number, and virus lysates were normalized according to RT activity. The upper and lower panels show APO3G proteins present in transfected HeLa cells (Cell) and in virions (Virus), respectively. The amount of CA protein in each virus sample is also shown. Lanes: 1, WT; 2, C100S; 3, C291S; 4, C100S/C291S; and 5, vector control.

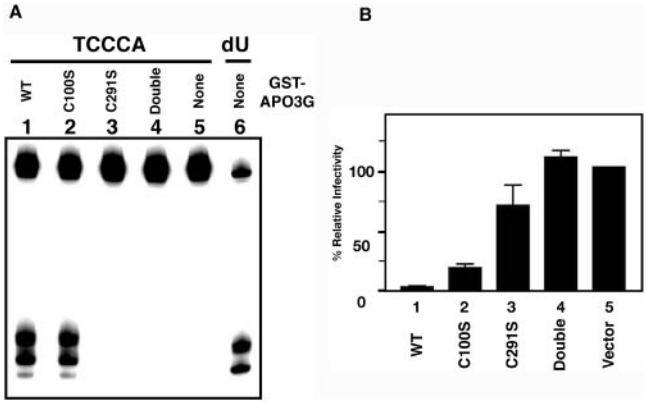

FIG. 7. Effect of zinc finger mutations on enzymatic and anti-HIV-1 activities of APO3G. (A) The effect of zinc finger mutations on the deaminase activity of APO3G was analyzed by the UDG-dependent deaminase assay. Substrate JL653 (containing the TCCCA motif) was incubated with WT (lane 1), C100S (lane 2), C291S (lane 3), or C100S/C291S (lane 4) GST-APO3G protein (each at 1.0 μM) or without any GST-APO3G protein (lane 5). The positive control, JL651 containing a dU residue (lane 6), was incubated only with UDG. (B) Antiviral effects of the zinc finger mutants. HeLa cells were cotransfected with HIV-1*vif*(−) plasmid DNA and a plasmid containing the coding sequence for WT APO3G (lane 1), C100S (lane 2), C291S (lane 3), and the double mutant (lane 4); vector pcDNA 3.1, control (lane 5). Two days posttransfection, virus-containing supernatants were normalized for equivalent amounts of RT activity and were assayed for infectivity. The data are expressed in a bar graph as the infectivity relative to the vector control, which was set at 100%. Note that since the transfection procedures as well as the amounts of HIV-1*vif*(−) plasmid DNA and the APO3G expression construct used for transfection in panel B were the same as those used for Fig. 6B, similar levels of protein should be expressed in both experiments.

pletely effective. Collectively, these data demonstrate that the second zinc finger is solely responsible for deaminase activity.

In light of these results, we wondered whether the antiviral effect of APO3G is a consequence of its deaminase activity. Until now, a consensus has not been reached. To address this issue, we investigated the antiviral activities of virions expressing WT or mutant APO3G. As shown in Fig. 7B, WT APO3G strongly suppressed virus infectivity (by 97%). In contrast, the double mutant had no antiviral effect (relative infectivity, 108%), in agreement with Newman et al. (31), presumably because the mutant protein is not encapsidated (Fig. 6B). The single mutants exhibited an intermediate response. Thus, the relative infectivity obtained with the C100S mutant was dramatically but not completely reduced (strong antiviral effect), with a measured value of 19% of the control. However, if the lower efficiency of C100S encapsidation is taken into account (Fig. 6B), the antiviral activity of this mutant approaches that of WT APO3G. In contrast, with the C291S mutant, the relative infectivity was considerable (67% of the control), consistent with a weak antiviral effect. These findings demonstrate that the second zinc finger domain is more important for antiviral activity than the first zinc finger domain and that a correlation exists between deaminase and antiviral activities.

DISCUSSION

Here, we present an in-depth molecular analysis of the nucleic acid binding and deaminase activities of APO3G, using highly purified, enzymatically active protein expressed in a baculovirus system. We find that the substrate specificity and nucleotide preferences differ for each of these activities. In addition, we demonstrate that the two zinc finger domains have different roles in nucleic acid binding, deamination, and antiviral activity. To our knowledge, this is the first detailed study of the properties of the purified protein. In addition, we show for the first time that purified GST-tagged and untagged APO3G have very similar activities.

Examination of the substrate specificity for deamination demonstrates that APO3G deaminates cytosines in ssDNA (Fig. 2B) (2, 15, 24, 26, 44, 51, 54) but not 5mC residues (Fig.

2C). From a structural point of view this seems reasonable, since the methyl group at position 5 of cytosine might hinder the interaction of the amino group at position 4 with the catalytic center of APO3G. Moreover, this suggests that there is likely to be a strict spatial requirement to accommodate the base being deaminated.

In addition to 5mC residues in ssDNA, cytosine residues in dsDNA, dsRNA, a DNA/RNA hybrid, or in ssRNA are also refractory to deamination by APO3G (Fig. 2). These findings are consistent with previous reports (44, 51) and with the results of sequencing genomic RNA (51, 54). However, we cannot exclude the possibility that another factor(s) might be required for intracellular deamination of RNA substrates, as in the case of APO1 (4, 48).

The role of each zinc finger domain in deamination was tested directly, and the results were unequivocal (Fig. 7A). Thus, the second zinc finger domain is solely responsible for deaminase activity and the first zinc finger domain does not modify this activity. This conclusion is in accord with other work (14, 30, 31). In two studies, however, it was found that mutations in the catalytic Glu residues (40) or in zinc-coordinating residues (54) from either domain exhibited a similar reduction in deaminase activity. The explanation for these discrepancies with our findings and those of others (14, 30, 31) is not clear.

The nature of the nucleic acid binding properties of APO3G is a major issue that we address, since the binding capacity is essential for encapsidation of APO3G into virions (22, 30, 37, 45, 53) and in all likelihood for antiviral activity as well. These studies were performed in vitro using purified enzyme, but it is possible that, in vivo, other factor(s) that could affect the binding properties of APO3G might also be involved. In the experiments presented here, the EMSA results show that APO3G binds to ssRNA or ssDNA with similar efficiency (Fig. 3A) (51). We also find that APO3G has a relatively high affinity for a DNA/RNA hybrid (~50% of the binding activity seen with ssDNA or ssRNA) (Fig. 3B), although a lower binding efficiency was observed when a GST-APO3G protein expressed in *E. coli* was used (51). The ability to bind to a DNA/RNA hybrid might allow APO3G to remain transiently bound to the hybrid formed during minus-strand DNA synthesis. Thus, as RNase H degrades genomic RNA, APO3G would be positioned to readily deaminate the resulting ssDNA.

Additionally, we find that APO3G prefers to bind to dT or dU residues in homopolymeric ssDNAs and only poorly to similar oligos containing dC or dA residues (Fig. 3C). Surprisingly, the *E. coli*-expressed GST-APO3G was reported to have a preference for binding to C-rich ssDNA and RNA oligos (51). The possibility that the *E. coli* protein might not fold into the proper native conformation might account for this apparent discrepancy. Although in vivo data are not available, it is noteworthy that the results obtained here (Fig. 3C) and in other experiments showing a preference for binding to a dAT-rich oligo compared with a dA-rich oligo (data not shown) are consistent with the preferred binding of baculovirus-expressed GST-APO3G (19) and APO1 (1, 29) to AU-rich ssRNA. Importantly, as is the case for APO1 (1, 29), our results also demonstrate that the nucleotide preferences and substrate specificities of purified APO3G differ for deaminase and nucleic acid binding activities (compare Fig. 2 and 3).

In other experiments, we show that APO3G binding to ssDNA in the EMSA is efficient as long as the nucleic acid is 16 nt or longer (Fig. 4). Our findings also suggest that the single-shifted band observed by EMSA with the 20-, 18-, or 16-nt ssDNA (Fig. 4) consists of a single uniform complex with the nucleic acid and APO3G. In addition, from these results it would appear that APO3G covers approximately 10 to 15 nt. Interestingly, a dimeric form of APO3G is detected when an 18-nt ssDNA-APO3G complex is chemically cross-linked (Y. Iwatani and J. G. Levin, unpublished observation). This is in accord with data indicating that APO3G can form oligomers with other APO3G molecules (19, 30, 32, 40, 49) as well as with APO3B (19) or APO3F (49). Moreover, pull-down experiments have shown that APO3G oligomerization is extremely sensitive to RNase, implying that nucleic acid plays a role in this process (32). Structural studies will be necessary to determine the exact nature of nucleic acid complexes formed with APO3G in its monomeric and oligomeric forms.

NC and APO3G are both nucleic acid binding proteins, yet NC does not affect deamination of an ssDNA oligo by purified APO3G (Fig. 2A). Moreover, when NC and APO3G are both present in the same reaction, analysis by EMSA demonstrates that neither protein interferes with the other's binding to RNA (either a 40-nt ssRNA oligo [Fig. 5A and B] or the biologically relevant 33-nt SL-3 RNA oligo [Fig. 5C and D]). Rather, a complex consisting of NC, APO3G, and RNA is formed. With the 40-nt ssRNA, binding does not appear to be cooperative, since NC does not affect the efficiency of APO3G binding and vice versa (Fig. 5A and B). Interestingly, in reactions with SL-3 RNA, NC promotes more efficient binding of APO3G to the stem-loop structure (Fig. 5C and D). This is presumably due to NC's nucleic acid chaperone activity, which allows NC to destabilize secondary structures (reviewed in reference 25). As a consequence, the RNA becomes a more suitable substrate for APO3G binding. Taken together, these findings strongly support the results of other studies showing that an RNA binding or "bridging" activity is required for APO3G packaging by the NC domain in Gag (30, 37, 53). The data are also consistent with an alternative model suggesting that the Gag-APO3G interaction is mediated by protein-RNA interactions as well as by a specific protein-protein interaction (7).

APO3G binding to nucleic acids is dependent on zinc coordination, and mutational analysis indicates that there are differences in the functions of each domain (Fig. 6 and 7). How can we rationalize our observation that the first zinc finger domain is more important for nucleic acid binding (Fig. 6) (30) while deaminase activity is associated only with the second zinc finger domain (Fig. 7A) (14, 30, 31)? Amino acid sequence analysis provides some explanation for the greater binding activity of the first zinc finger domain. For example, the sequence motif of the first zinc finger (36 residues) contains eight positively charged (Arg, Lys, and His) amino acids, while zinc finger two (35 residues) has only two. Based on computer analysis, we estimate that the pI of the N-terminal half of APO3G (residues 1 to 188) is 9.63, whereas the value for the C-terminal domain (residues 189 to 384) is 5.90. These differences in amino acid charge would be expected to affect the nucleic acid binding activity of the two domains. In addition, it is known that aromatic amino acids found within nucleic acid binding proteins are often essential for binding activity (e.g.,

APO1 [29], APO3G [30], and NC [25]). Thus, in APO3G, the first zinc finger domain contains nine aromatic amino acids (enriched for Trp compared to zinc finger two), while the second zinc finger domain has seven. Taken together, these considerations reinforce the conclusion that the two zinc finger domains are not equivalent (18). Presumably, different folding of the two domains accounts for the exclusive presence of a functional catalytic center in the second zinc finger.

A critical aspect of APO3G's biological activity is its ability to strongly inhibit HIV-1 infectivity in the absence of Vif. We have asked a key question: Is the antiviral effect a consequence of APO3G's deaminase activity or is another mechanism involved? One approach has been to study the effects of point mutations in the zinc finger domains. A number of investigators have found that deamination is linked to antiviral activity (26, 30, 40, 54), although there has been disagreement over whether both zinc finger domains (26, 54) or primarily the second domain (30, 40) is involved. In contrast, in a recent study it was reported that point mutations in either the first or second domain had similar inhibitory effects on antiviral activity. These findings led to the proposal that the antiviral function of APO3G can be dissociated from deaminase activity and that some other mechanism, as yet undefined, is responsible for antiviral activity (31). These authors, who used untagged proteins for their work, suggested that conflicting data obtained by others might result from the use of epitope-tagged proteins, which could interfere with mutant APO3G expression and function (31). However, one of us (K. Strebel) has found that epitope-tagged and untagged WT or mutant APO3G have equivalent activities in a cell-based system (32). It is possible that these disparate results concerning antiviral activity reflect differences in experimental protocols, which would affect APO3G expression and/or encapsidation into virions.

In the present study, our results indicate that deamination is correlated with APO3G's antiviral effect. Thus, the second zinc finger domain, which contains the active site for deamination (Fig. 7A), is more important than domain one with respect to antiviral activity (Fig. 7B). However, we cannot rule out some contribution from the first zinc finger domain. If deamination indeed plays a crucial role in promoting the antiviral effect, it raises the important question of what mechanism is used by APO3G to block HIV-1 reverse transcription (12, 41, 47) and, ultimately, viral infectivity. Extensive G-to-A hypermutation in plus-strand DNA and possible degradation of DNA with abasic residues (reviewed in references 6, 11, 16, and 21) as well as a decrease in the specificity of plus-strand initiation (23) can result from deamination and potentially have a detrimental effect on virus replication.

In summary, we have described the molecular properties of purified human APO3G and have demonstrated their relation to APO3G's antiviral activity. The results demonstrate that the second zinc finger domain, which we show contains the active site for deaminase activity, has a major role in the antiviral effect of APO3G and thus support a mechanism for antiviral activity that involves deamination.

ACKNOWLEDGMENTS

We thank Robert J. Crouch and Sergey Gaidamakov for assistance with the purification of APO3G as well as for helpful discussions. We are also indebted to Robert J. Gorelick for his generous gift of recombinant NC protein, Alan Rein for critical reading of the manuscript, and Tiyun Wu for gracious assistance with preparation of the figures.

This research was supported by the Intramural Research Program of the NIH (NICHD and NIAID).

REFERENCES

1. **Anant, S., and N. O. Davidson.** 2000. An AU-rich sequence element (UUUN[A/U]U) downstream of the edited C in apolipoprotein B mRNA is a high-affinity binding site for Apobec-1: binding of Apobec-1 to this motif in the 3′ untranslated region of c-myc increases mRNA stability. Mol. Cell. Biol. **20:**1982–1992.
2. **Beale, R. C., S. K. Petersen-Mahrt, I. N. Watt, R. S. Harris, C. Rada, and M. S. Neuberger.** 2004. Comparison of the differential context-dependence of DNA deamination by APOBEC enzymes: correlation with mutation spectra in vivo. J. Mol. Biol. **337:**585–596.
3. **Bhattacharya, S., N. Navaratnam, J. R. Morrison, J. Scott, and W. R. Taylor.** 1994. Cytosine nucleoside/nucleotide deaminases and apolipoprotein B mRNA editing. Trends Biochem. Sci. **19:**105–106.
4. **Chester, A., J. Scott, S. Anant, and N. Navaratnam.** 2000. RNA editing: cytidine to uridine conversion in apolipoprotein B mRNA. Biochim. Biophys. Acta **1494:**1–13.
5. **Conticello, S. G., R. S. Harris, and M. S. Neuberger.** 2003. The Vif protein of HIV triggers degradation of the human antiretroviral DNA deaminase APOBEC3G. Curr. Biol. **13:**2009–2013.
6. **Cullen, B. R.** 2003. HIV-1 Vif: counteracting innate antiretroviral defenses. Mol. Ther. **8:**525–527.
7. **Cullen, B. R.** 2006. Role and mechanism of action of the APOBEC3 family of antiretroviral resistance factors. J. Virol. **80:**1067–1076.
8. **Fisher, A. G., B. Ensoli, L. Ivanoff, M. Chamberlain, S. Petteway, L. Ratner, R. C. Gallo, and F. Wong-Staal.** 1987. The *sor* gene of HIV-1 is required for efficient virus transmission in vitro. Science **237:**888–893.
9. **Fouchier, R. A., J. H. Simon, A. B. Jaffe, and M. H. Malim.** 1996. Human immunodeficiency virus type 1 Vif does not influence expression or virion incorporation of *gag*-, *pol*-, and *env*-encoded proteins. J. Virol. **70:**8263–8269.
10. **Gabuzda, D. H., K. Lawrence, E. Langhoff, E. Terwilliger, T. Dorfman, W. A. Haseltine, and J. Sodroski.** 1992. Role of *vif* in replication of human immunodeficiency virus type 1 in $CD4^+$ T lymphocytes. J. Virol. **66:**6489–6495.
11. **Goff, S. P.** 2003. Death by deamination: a novel host restriction system for HIV-1. Cell **114:**281–283.
12. **Goncalves, J., Y. Korin, J. Zack, and D. Gabuzda.** 1996. Role of Vif in human immunodeficiency virus type 1 reverse transcription. J. Virol. **70:**8701–8709.
13. **Guo, J., W. Wu, Z. Y. Yuan, K. Post, R. J. Crouch, and J. G. Levin.** 1995. Defects in primer-template binding, processive DNA synthesis, and RNase H activity associated with chimeric reverse transcriptases having the murine leukemia virus polymerase domain joined to *Escherichia coli* RNase H. Biochemistry **34:**5018–5029.
14. **Haché, G., M. T. Liddament, and R. S. Harris.** 2005. The retroviral hypermutation specificity of APOBEC3F and APOBEC3G is governed by the C-terminal DNA cytosine deaminase domain. J. Biol. Chem. **280:**10920–10924.
15. **Harris, R. S., K. N. Bishop, A. M. Sheehy, H. M. Craig, S. K. Petersen-Mahrt, I. N. Watt, M. S. Neuberger, and M. H. Malim.** 2003. DNA deamination mediates innate immunity to retroviral infection. Cell **113:**803–809.
16. **Harris, R. S., A. M. Sheehy, H. M. Craig, M. H. Malim, and M. S. Neuberger.** 2003. DNA deamination: not just a trigger for antibody diversification but also a mechanism for defense against retroviruses. Nat. Immunol. **4:**641–643.
17. **Henderson, L. E., M. A. Bowers, R. C. Sowder II, S. A. Serabyn, D. G. Johnson, J. W. Bess, Jr., L. O. Arthur, D. K. Bryant, and C. Fenselau.** 1992. Gag proteins of the highly replicative MN strain of human immunodeficiency virus type 1: posttranslational modifications, proteolytic processings, and complete amino acid sequences. J. Virol. **66:**1856–1865.
18. **Huthoff, H., and M. H. Malim.** 2005. Cytidine deamination and resistance to retroviral infection: towards a structural understanding of the APOBEC proteins. Virology **334:**147–153.
19. **Jarmuz, A., A. Chester, J. Bayliss, J. Gisbourne, I. Dunham, J. Scott, and N. Navaratnam.** 2002. An anthropoid-specific locus of orphan C to U RNA-editing enzymes on chromosome 22. Genomics **79:**285–296.
20. **Kao, S., M. A. Khan, E. Miyagi, R. Plishka, A. Buckler-White, and K. Strebel.** 2003. The human immunodeficiency virus type 1 Vif protein reduces intracellular expression and inhibits packaging of APOBEC3G (CEM15), a cellular inhibitor of virus infectivity. J. Virol. **77:**11398–11407.
21. **KewalRamani, V. N., and J. M. Coffin.** 2003. Weapons of mutational destruction. Science **301:**923–925.
22. **Khan, M. A., S. Kao, E. Miyagi, H. Takeuchi, R. Goila-Gaur, S. Opi, C. L. Gipson, T. G. Parslow, H. Ly, and K. Strebel.** 2005. Viral RNA is required for the association of APOBEC3G with human immunodeficiency virus type 1 nucleoprotein complexes. J. Virol. **79:**5870–5874.
23. **Klarmann, G. J., X. Chen, T. W. North, and B. D. Preston.** 2003. Incorporation of uracil into minus strand DNA affects the specificity of plus strand

synthesis initiation during lentiviral reverse transcription. J. Biol. Chem. **278:**7902–7909.
24. **Lecossier, D., F. Bouchonnet, F. Clavel, and A. J. Hance.** 2003. Hypermutation of HIV-1 DNA in the absence of the Vif protein. Science **300:**1112.
25. **Levin, J. G., J. Guo, I. Rouzina, and K. Musier-Forsyth.** 2005. Nucleic acid chaperone activity of HIV-1 nucleocapsid protein: critical role in reverse transcription and molecular mechanism. Prog. Nucleic Acid Res. Mol. Biol. **80:**217–286.
26. **Mangeat, B., P. Turelli, G. Caron, M. Friedli, L. Perrin, and D. Trono.** 2003. Broad antiretroviral defence by human APOBEC3G through lethal editing of nascent reverse transcripts. Nature **424:**99–103.
27. **Marin, M., K. M. Rose, S. L. Kozak, and D. Kabat.** 2003. HIV-1 Vif protein binds the editing enzyme APOBEC3G and induces its degradation. Nat. Med. **9:**1398–1403.
28. **Mehle, A., B. Strack, P. Ancuta, C. Zhang, M. McPike, and D. Gabuzda.** 2004. Vif overcomes the innate antiviral activity of APOBEC3G by promoting its degradation in the ubiquitin-proteasome pathway. J. Biol. Chem. **279:**7792–7798.
29. **Navaratnam, N., S. Bhattacharya, T. Fujino, D. Patel, A. L. Jarmuz, and J. Scott.** 1995. Evolutionary origins of *apoB* mRNA editing: catalysis by a cytidine deaminase that has acquired a novel RNA-binding motif at its active site. Cell **81:**187–195.
30. **Navarro, F., B. Bollman, H. Chen, R. König, Q. Yu, K. Chiles, and N. R. Landau.** 2005. Complementary function of the two catalytic domains of APOBEC3G. Virology **333:**374–386.
31. **Newman, E. N. C., R. K. Holmes, H. M. Craig, K. C. Klein, J. R. Lingappa, M. H. Malim, and A. M. Sheehy.** 2005. Antiviral function of APOBEC3G can be dissociated from cytidine deaminase activity. Curr. Biol. **15:**166–170.
32. **Opi, S., H. Takeuchi, S. Kao, M. A. Khan, E. Miyagi, R. Goila-Gaur, Y. Iwatani, J. G. Levin, and K. Strebel.** 2006. Monomeric APOBEC3G is catalytically active and has antiviral activity. J. Virol. **80:**4673–4682.
33. **Robertson, K. D., and A. P. Wolffe.** 2000. DNA methylation in health and disease. Nat. Rev. Genet. **1:**11–19.
34. **Roos, J. W., M. F. Maughan, Z. Liao, J. E. K. Hildreth, and J. E. Clements.** 2000. LuSIV cells: a reporter cell line for the detection and quantitation of a single cycle of HIV and SIV replication. Virology **273:**307–315.
35. **Russell, R. S., C. Liang, and M. A. Wainberg.** 2004. Is HIV-1 RNA dimerization a prerequisite for packaging? Yes, no, probably? Retrovirology **1:**23.
36. **Sakai, H., R. Shibata, J. Sakuragi, S. Sakuragi, M. Kawamura, and A. Adachi.** 1993. Cell-dependent requirement of human immunodeficiency virus type 1 Vif protein for maturation of virus particles. J. Virol. **67:**1663–1666.
37. **Schäfer, A., H. P. Bogerd, and B. R. Cullen.** 2004. Specific packaging of APOBEC3G into HIV-1 virions is mediated by the nucleocapsid domain of the gag polyprotein precursor. Virology **328:**163–168.
38. **Sheehy, A. M., N. C. Gaddis, J. D. Choi, and M. H. Malim.** 2002. Isolation of a human gene that inhibits HIV-1 infection and is suppressed by the viral Vif protein. Nature **418:**646–650.
39. **Sheehy, A. M., N. C. Gaddis, and M. H. Malim.** 2003. The antiretroviral enzyme APOBEC3G is degraded by the proteasome in response to HIV-1 Vif. Nat. Med. **9:**1404–1407.
40. **Shindo, K., A. Takaori-Kondo, M. Kobayashi, A. Abudu, K. Fukunaga, and T. Uchiyama.** 2003. The enzymatic activity of CEM15/Apobec-3G is essential for the regulation of the infectivity of HIV-1 virion but not a sole determinant of its antiviral activity. J. Biol. Chem. **278:**44412–44416.
41. **Sova, P., and D. J. Volsky.** 1993. Efficiency of viral DNA synthesis during infection of permissive and nonpermissive cells with *vif*-negative human immunodeficiency virus type 1. J. Virol. **67:**6322–6326.
42. **Stopak, K., C. de Noronha, W. Yonemoto, and W. C. Greene.** 2003. HIV-1 Vif blocks the antiviral activity of APOBEC3G by impairing both its translation and intracellular stability. Mol. Cell **12:**591–601.
43. **Strebel, K., D. Daugherty, K. Clouse, D. Cohen, T. Folks, and M. A. Martin.** 1987. The HIV 'A' (sor) gene product is essential for virus infectivity. Nature **328:**728–730.
44. **Suspène, R., P. Sommer, M. Henry, S. Ferris, D. Guétard, S. Pochet, A. Chester, N. Navaratnam, S. Wain-Hobson, and J.-P. Vartanian.** 2004. APOBEC3G is a single-stranded DNA cytidine deaminase and functions independently of HIV reverse transcriptase. Nucleic Acids Res. **32:**2421–2429.
45. **Svarovskaia, E. S., H. Xu, J. L. Mbisa, R. Barr, R. J. Gorelick, A. Ono, E. O. Freed, W.- S. Hu, and V. K. Pathak.** 2004. Human apolipoprotein B mRNA-editing enzyme-catalytic polypeptide-like 3G (APOBEC3G) is incorporated into HIV-1 virions through interactions with viral and nonviral RNAs. J. Biol. Chem. **279:**35822–35828.
46. **Takeuchi, H., S. Kao, E. Miyagi, M. A. Khan, A. Buckler-White, R. Plishka, and K. Strebel.** 2005. Production of infectious SIVagm from human cells requires functional inactivation but not viral exclusion of human APOBEC3G. J. Biol. Chem. **280:**375–382.
47. **von Schwedler, U., J. Song, C. Aiken, and D. Trono.** 1993. *vif* is crucial for human immunodeficiency virus type 1 proviral DNA synthesis in infected cells. J. Virol. **67:**4945–4955.
48. **Wedekind, J. E., G. S. Dance, M. P. Sowden, and H. C. Smith.** 2003. Messenger RNA editing in mammals: new members of the APOBEC family seeking roles in the family business. Trends Genet. **19:**207–216.
49. **Wiegand, H. L., B. P. Doehle, H. P. Bogerd, and B. R. Cullen.** 2004. A second human antiretroviral factor, APOBEC3F, is suppressed by the HIV-1 and HIV-2 Vif proteins. EMBO J. **23:**2451–2458.
50. **Wu, W., L. E. Henderson, T. D. Copeland, R. J. Gorelick, W. J. Bosche, A. Rein, and J. G. Levin.** 1996. Human immunodeficiency virus type 1 nucleocapsid protein reduces reverse transcriptase pausing at a secondary structure near the murine leukemia virus polypurine tract. J. Virol. **70:**7132–7142.
51. **Yu, Q., R. König, S. Pillai, K. Chiles, M. Kearney, S. Palmer, D. Richman, J. M. Coffin, and N. R. Landau.** 2004. Single-strand specificity of APOBEC3G accounts for minus-strand deamination of the HIV genome. Nat. Struct. Mol. Biol. **11:**435–442.
52. **Yu, X., Y. Yu, B. Liu, K. Luo, W. Kong, P. Mao, and X.-F. Yu.** 2003. Induction of APOBEC3G ubiquitination and degradation by an HIV-1 Vif-Cul5-SCF complex. Science **302:**1056–1060.
53. **Zennou, V., D. Perez-Caballero, H. Göttlinger, and P. D. Bieniasz.** 2004. APOBEC3G incorporation into human immunodeficiency virus type 1 particles. J. Virol. **78:**12058–12061.
54. **Zhang, H., B. Yang, R. J. Pomerantz, C. Zhang, S. C. Arunachalam, and L. Gao.** 2003. The cytidine deaminase CEM15 induces hypermutation in newly synthesized HIV-1 DNA. Nature **424:**94–98.